Supplementary Information

Information Type	Description
Supplementary Discussion and Study Limitations	Additional discussion, including study limitations.
Supplementary Fig. 1	Gating strategy for the Cytek 36-color flow cytometry panel run on peripheral blood mononuclear cells.
Supplementary Fig. 2	Gene expression profile of antigen presentation, NF-κB/inflammatory, and monocytic myeloid-derived suppressor cell (MDSC) related signatures in classical monocytes.
Supplementary Fig. 3	Gating strategies for the Cytek B-cell-centric flow-cytometry panel: showing the gating of influenza-specific plasmablast populations.
Supplementary Fig. 4	Multivariate elastic net models identifying baseline cell subsets that contribute to predicting day 1 IFNγ responses.
Supplementary Fig. 5	Additional supporting data for IFNγ responses by subsets of CD8+ EM T-cells.
Supplementary Fig. 6	Flow cytometry analyses of *in vitro* cytokine stimulation of baseline PBMCs (D0 before influenza vaccination).
Supplementary Fig. 7	Additional cell subsets that potentially contribute to the increased day 1 IFNγ responses in COVID-19-recovered males.
Supplementary Table 1	Baseline parameter TSD association results (all subjects)
Supplementary Table 2	Baseline parameter DE results (all subjects)
Supplementary Table 3	Baseline whole blood GSEA results (all subjects)
Supplementary Table 4	Significant ($p < 0.05$) single cell timepoint DE results
Supplementary Table 5	Timepoint whole blood and single cell GSEA results
Supplementary Table 6	Zhai *et al* natural influenza infection cohort DE results
Supplementary Table 7	Post-influenza vaccination timepoint DE results
Supplementary Table 8	Influenza vaccine antibody titer and SPR D0 and D28 model results
Supplementary Table 9	Gated populations in 36-color Cytek panel
Supplementary Table 10	COVR-M CD8 EM Markers from CITE-seq
Supplementary Table 11	Protein surface marker panel used for CITE-seq, Biolegend Total-seq-C Human Universal Cocktail, V1.0
Supplementary Table 12	Antibodies and influenza probes used in B-cell flow panel
Supplementary Table 13	Antibodies and viability dyes used in 36-color Cytek flow cytometry panel
Supplementary Table 14	Antibodies and viability dyes used in T-cell stimulation assays

Supplementary Information: Supplementary Discussion and Study Limitations

Some of the sex dimorphic imprints we identified might be attributable to differences in acute disease severity (e.g., males tend to have more severe disease than females[1,2]). However, it is not clear how that might have manifested in our mild, non-hospitalized patients as neither the self-reported duration of acute illness nor antibody titers against SARS-CoV-2 were different between COVR-M and COVR-F (duration of illness Wilcoxon p=0.37; USA-WA1 IC_{50} Wilcoxon p=0.26), which together suggest that our observations are potentially independent of severity or immune response quality during acute disease.

Innate "priming" effect has been observed in repeated homologous vaccination, such as increased innate responses following the second dose of the Pfizer-BioNTech COVID-19 vaccine or the AS01-adjuvanted hepatitis B vaccine compared to the first dose[3,4]. It remains to be seen whether similar, non-antigen specific virtual memory CD8 EM T-cells are involved, particularly given that these homologous (repeated dosing) vaccine-induced responses did not appear to be sex-specific and the second dose was given only 3-4 weeks after the first, compared to the months between mild COVID-19 and influenza vaccination in our study.

Changes in the transcriptional and epigenetic profiles of peripheral monocytes have been described in both acute and convalescent COVID-19 patients with moderate-to-severe disease, but few included patients months out from infection[5–10]. These previously described changes during acute disease include depressed inflammation/antigen-presentation transcriptional phenotypes but are distinct from the monocyte depression signature involving TLRs that we detected months post COVID-19. The monocyte imprint we described involved transcriptionally depressed innate defense/receptor genes is also consistent with the notion of trained innate immunity[11]. However, our signature likely reflects different biology than the "poised" trained monocytes (based on epigenetic and *in vitro* stimulation studies) found in an earlier study of seven COVID-19-recovered patients, probably because those were hospitalized patients with severe acute disease (e.g., most had pneumonia) and the time since discharge was relatively short (~4-12 weeks)[9]. Our signature was also distinct from the other depressed antigen presentation or myeloid suppressor cell like states found in acute COVID-19. The finding that the innate immune receptor imprint we detected in monocytes can be shifted by seasonal

influenza vaccination towards the baseline of healthy individuals suggests that in addition to providing antigen-specific protection, vaccines could help establish stable immune cell statuses in an antigen-agnostic manner. However, the functional relevance of this partial reversal remains to be determined.

Limitations of this study

Most study subjects were younger than 65 and thus these findings may not apply to the elderly. Some of the imprints considered as stable given lack of association with TSD may still be evolving slowly; similarly, it is possible that some of the post-vaccination shift towards the healthy, pre-vaccination state by D28 may reflect ongoing disease resolution. However, this is unlikely the case for the vaccine-induced elevation in the expression of the shifted genes towards the healthy state because those changes were clearly detectable on D1 after vaccination and persisted through D28, especially in females, indicating that this shift was driven (or at least accelerated) by vaccination and could not be attributed to the "natural" resolution process alone.

While individual exposure history beyond prior COVID-19 can play a role in shaping the responses to influenza vaccination at the individual level, our study design comparatively assessed imprints at the group level. We enrolled, from the same geographic region, COVID-19-recovered subjects together with matching HCs who never had COVID-19 at the time of influenza vaccination. It is reasonable to assume that the extent of heterogeneity in the exposure history within each group is, on average, quite comparable between the COVR and matched HC groups. Thus, the group level features shared across individuals (e.g., depressed monocyte signatures or the heightened IFN response after influenza vaccination in COVR-M) are likely largely independent of differences in personal exposure history.

Logistical and pandemic-related challenges prevented us from enrolling and longitudinally following individuals starting from earlier time-points from acute COVID-19 through influenza vaccination, but future work could further evaluate the relationship between acute immune responses to COVID-19 and the long-term imprints revealed in this study within the same individuals. At the time of the study, the COVID-19 vaccine was not yet available and

circulating viruses were limited due social distancing and face mask adherence in the local area[13,14]; this makes us more confident that the observed immunological changes were due to COVID-19 and not attributable to other vaccines or viral infections between acute COVID-19 and influenza vaccination. While it would be informative to further assess our findings in follow up cohorts, given our observation that vaccination could perturb some of the immune imprints associated with prior mild COVID-19, identification and recruitment of a sufficient number of individuals who have not had a viral infection or COVID-19 vaccines since their COVID-19 disease would be impractical. Our study is thus unique in allowing us to dissect the immune imprints in healthy recoverees following the first wave of COVID-19 without apparent interference from perturbations between acute disease and influenza vaccination, including COVID-19 and other vaccines. Finally, the functional and clinical implications of the vaccine-induced partial reversal of the depressed gene signatures in monocytes remain to be determined.

The influenza vaccine was selected for this study due to its public health importance and well understood immune response dynamics in blood that permitted sample collection at the most informative time points post-vaccination. While previous exposure to influenza vaccination and/or natural infection complicates interpretation of antibody responses, we accounted for existing influenza antibody titers in the analyses. Administration of a vaccine antigen to which study participants were naïve (e.g., rabies vaccine) would have removed potential confounding due to prior influenza exposures, but the response dynamics to these vaccines are less well characterized and there was no public health indication to administer these vaccines. Tissue-level or lymph node responses were not assessed in our study due to logistical and clinical challenges, especially during the first wave of the pandemic in 2020 but can provide additional important insights.

References

1. Ursin, R. L. & Klein, S. L. Sex Differences in Respiratory Viral Pathogenesis and Treatments. *Annu. Rev. Virol.* **8**, 393–414 (2021).
2. Takahashi, T. & Iwasaki, A. Sex differences in immune responses. *Science* **371**, 347–348 (2021).

3. Arunachalam, P. S. *et al.* Systems vaccinology of the BNT162b2 mRNA vaccine in humans. *Nature* **596**, 410–416 (2021).
4. De Mot, L. D. *et al.* Transcriptional profiles of adjuvanted hepatitis B vaccines display variable interindividual homogeneity but a shared core signature. *Sci. Transl. Med.* (2020) doi:10.1126/scitranslmed.aay8618.
5. Brauns, E. *et al.* Functional reprogramming of monocytes in acute and convalescent severe COVID-19 patients. *available at Research Square https://doi.org/10.21203/rs.3.rs-766032/v1.* (2021).
6. Paludan, S. R. & Mogensen, T. H. Innate immunological pathways in COVID-19 pathogenesis. *Sci. Immunol.* (2022) doi:10.1126/sciimmunol.abm5505.
7. Schulte-Schrepping, J. *et al.* Severe COVID-19 Is Marked by a Dysregulated Myeloid Cell Compartment. *Cell* **182**, 1419-1440.e23 (2020).
8. Utrero-Rico, A. *et al.* Alterations in Circulating Monocytes Predict COVID-19 Severity and Include Chromatin Modifications Still Detectable Six Months after Recovery. *Biomedicines* **9**, 1253 (2021).
9. You, M. *et al.* Single-cell epigenomic landscape of peripheral immune cells reveals establishment of trained immunity in individuals convalescing from COVID-19. *Nat. Cell Biol.* **23**, 620–630 (2021).
10. Cheong, J.-G. *et al.* Epigenetic Memory of COVID-19 in Innate Immune Cells and Their Progenitors. 2022.02.09.479588 Preprint at https://doi.org/10.1101/2022.02.09.479588 (2022).
11. Netea, M. G. *et al.* Defining trained immunity and its role in health and disease. *Nat. Rev. Immunol.* **20**, 375–388 (2020).
12. Klein, S. L. & Flanagan, K. L. Sex differences in immune responses. *Nat. Rev. Immunol.* **16**, 626–638 (2016).
13. Qi, Y., Shaman, J. & Pei, S. Quantifying the Impact of COVID-19 Nonpharmaceutical Interventions on Influenza Transmission in the United States. *J. Infect. Dis.* **224**, 1500–1508 (2021).
14. Olsen, S. J. *et al.* Changes in Influenza and Other Respiratory Virus Activity During the COVID-19 Pandemic - United States, 2020-2021. *MMWR Morb. Mortal. Wkly. Rep.* **70**, 1013–1019 (2021).

Supplementary Fig. 1

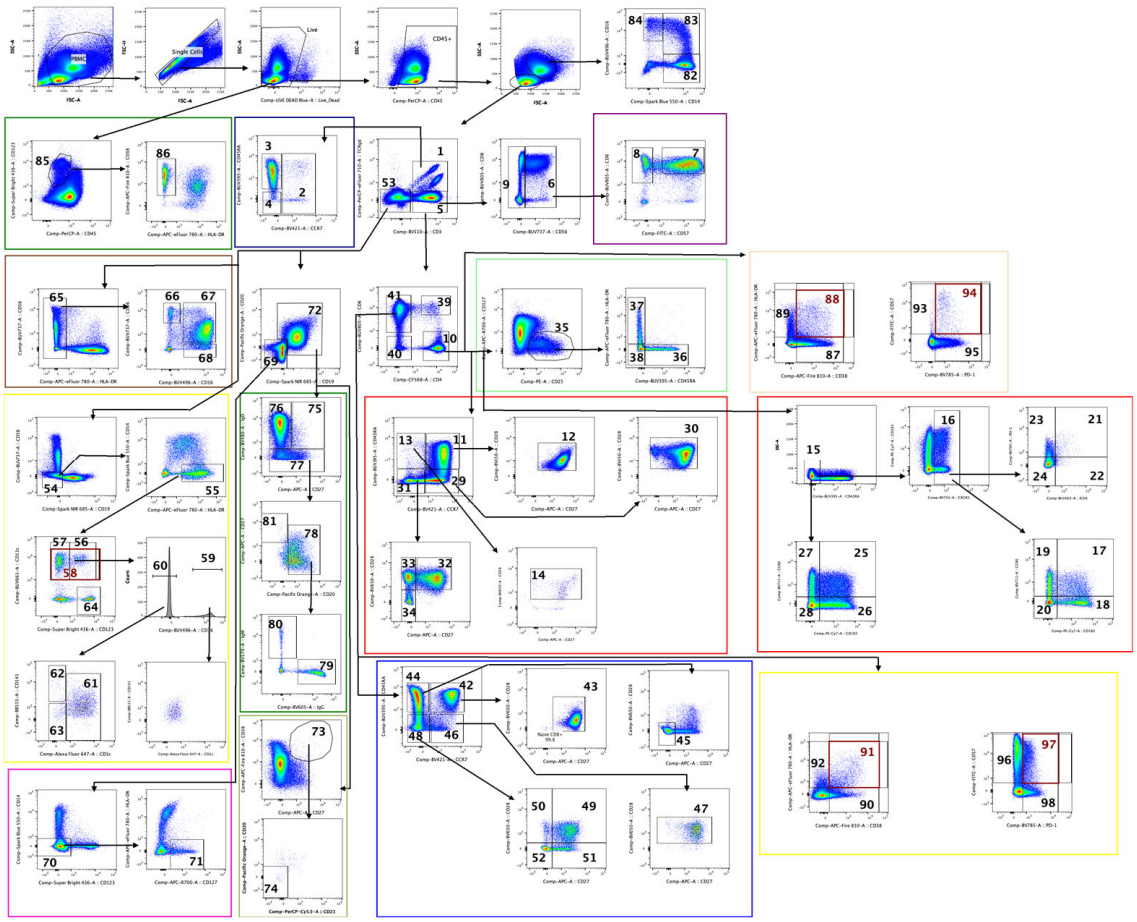

Supplementary Figure 1. Gating strategy for the Cytek 36-color flow cytometry panel run on peripheral blood mononuclear cells.

Supplementary Fig. 2

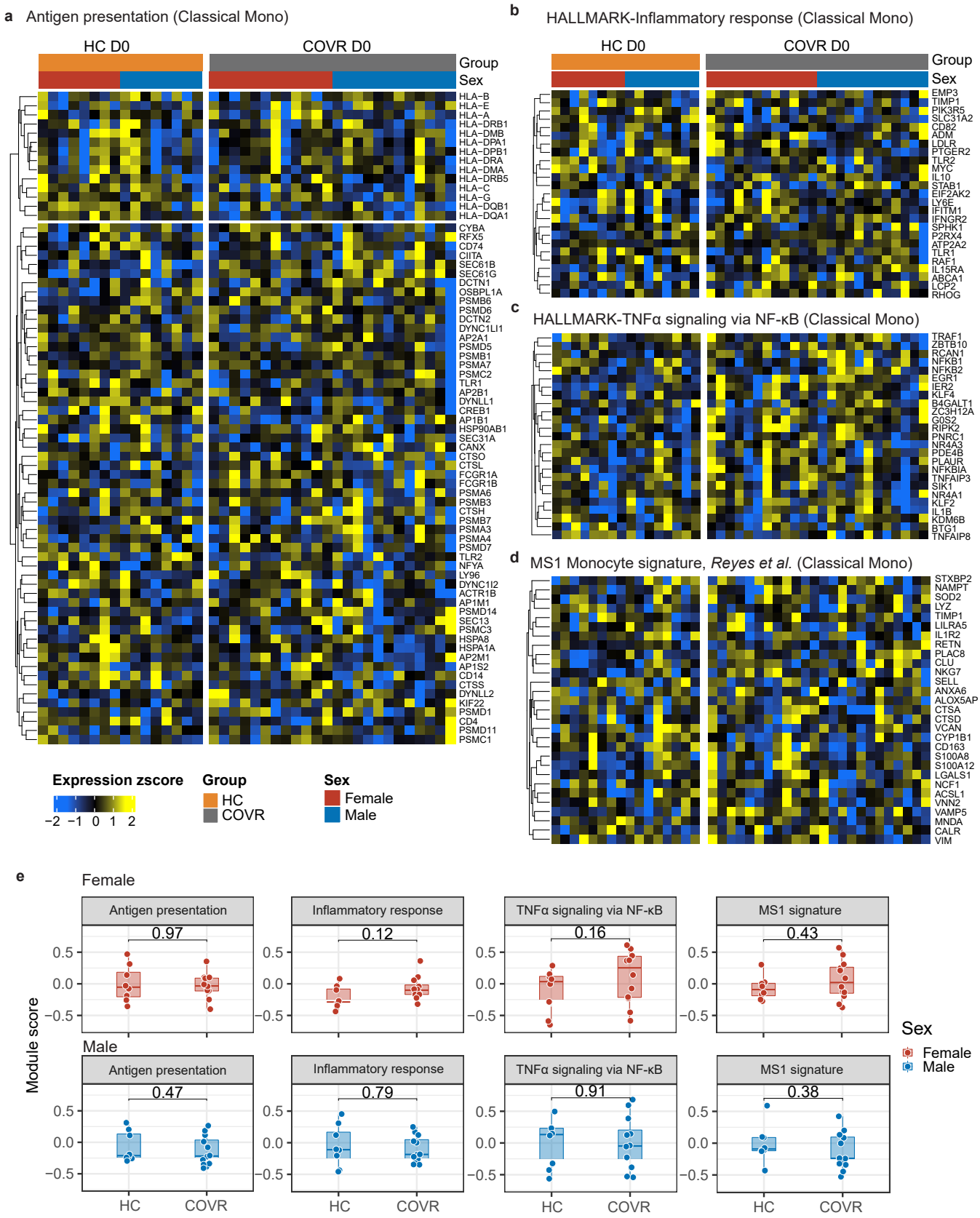

Supplementary Figure 2. Gene expression profile of antigen presentation, NF-κB/inflammatory, and monocytic myeloid-derived suppressor cell (MDSC) related signatures in classical monocytes

a, Heatmap showing the pseudobulk expression of the leading-edge genes (LEGs) from antigen presentation related gene sets, separately for male (M) and female (F), in classical monocytes from the CITE-seq day 0 (D0) pseudobulk data. The LEGs are from the acute COVID-19 vs. healthy control (HC) GSEA analysis in Liu *et al*[15], which showed that genes in the antigen presentation gene sets (KEGG Antigen processing and presentation, Reactome Antigen processing-Cross presentation, and Reactome MHC class II antigen presentation) tend to be lower in COVID-19. Samples (columns) are grouped by sex and subject group [HC at D0 and COVID-19-recovered (COVR) at D0 as indicated by the bars above the heatmap]. Gene names are shown on the right.

b, Similar to **(a)**, but showing the LEGs of the "Hallmark Inflammatory response" gene set.

c, Similar to **(a)**, but showing the LEGs of the "Hallmark TNFα signaling via NF-κB" gene set derived from the acute COVID-19 vs. HC GSEA analysis in Liu *et al*[15].

d, Similar to **(a)**, but showing the genes of MSDC/MS1 monocyte signature from Reyes *et al*[17]. **e,** Box plots showing the module scores of the LEGs of the gene sets in (**a-d**) separately for F (top row) and M (bottom row) for the indicated subject groups (columns), in classical monocytes from the CITE-seq D0 pseudobulk data. Each dot represents a sample. P values shown are from two-tailed Wilcoxon tests of the indicated two group comparisons.

Supplementary Fig. 3

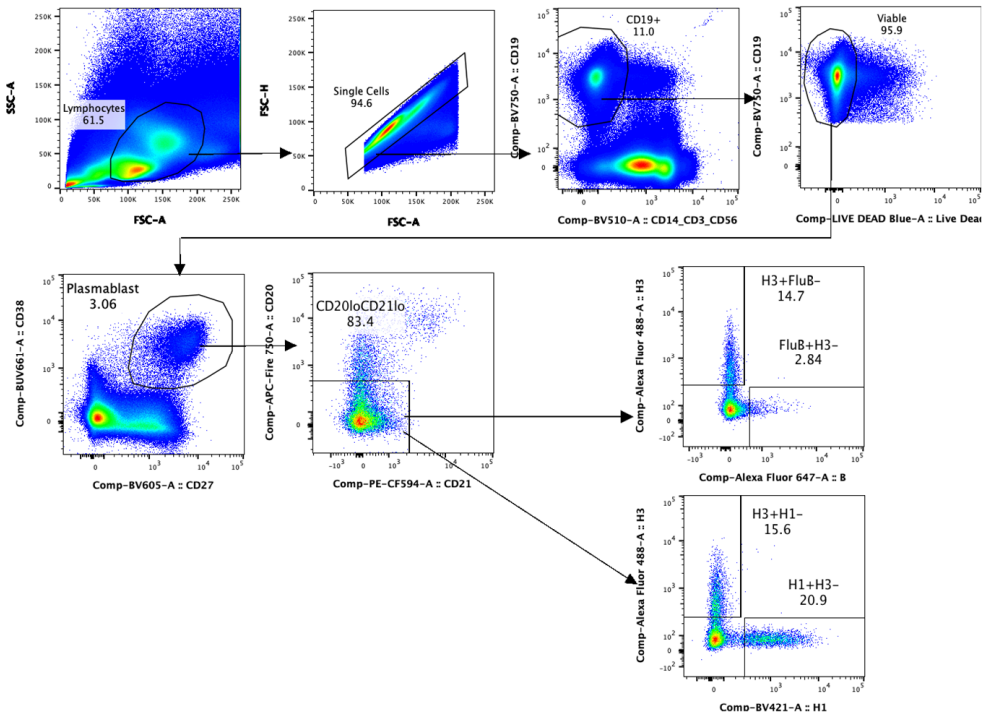

Supplementary Figure 3. Gating strategies for the Cytek B-cell-centric flow-cytometry panel: showing the gating of influenza-specific plasmablast populations.

Supplementary Fig. 4

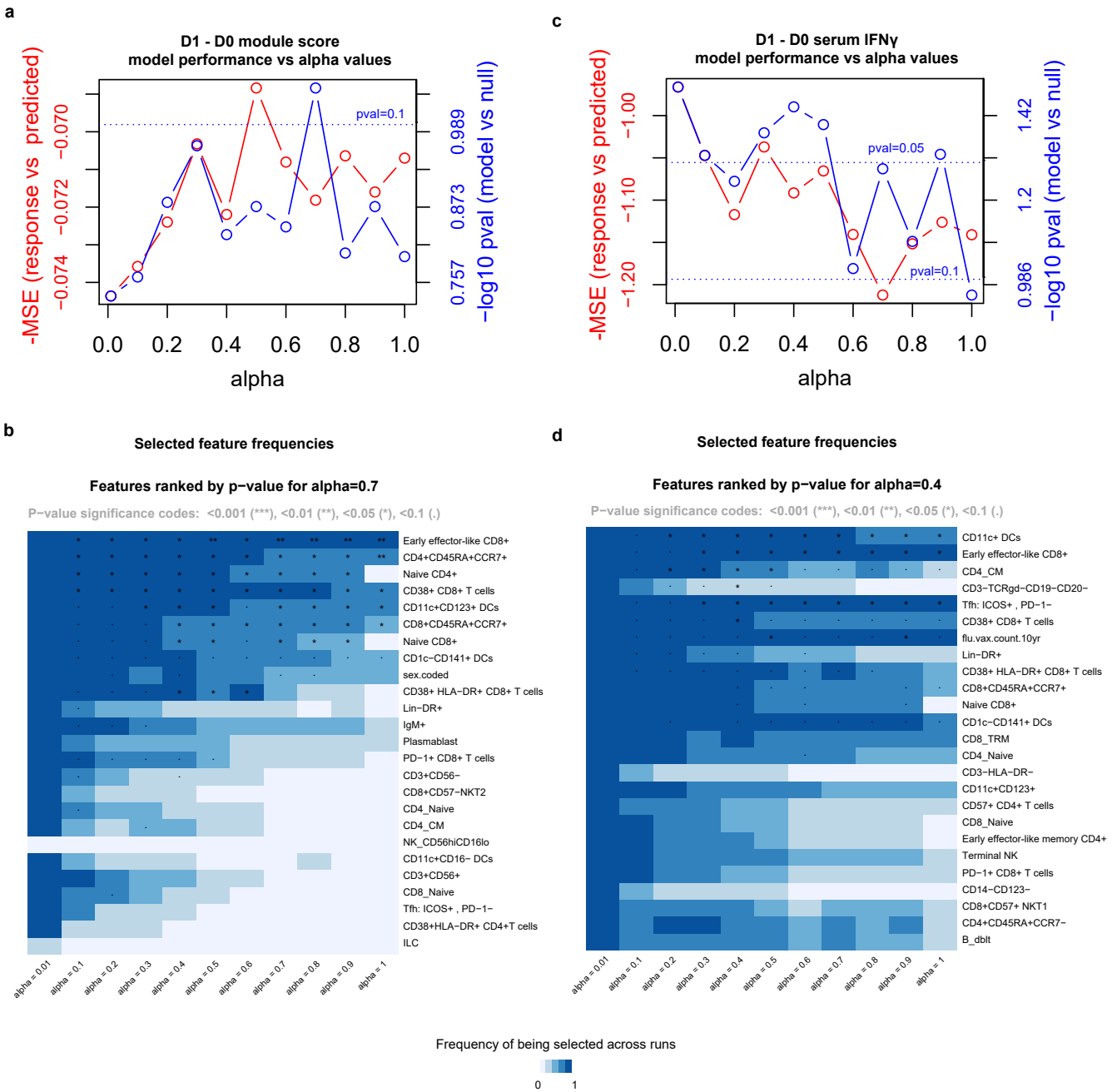

Supplementary Fig. 4. Multivariate elastic net models identifying baseline cell subsets that contribute to predicting day 1 IFNγ responses.

a, Elastic net model performance, as a function of the alpha parameter (tuning between lasso and ridge regression), for predicting the whole blood D1 – D0 Hallmark Interferon Gamma (IFNγ) Response module score. The red line represents the negative mean squared errors (-MSE; left y-axis) of the predicted values from the true responses across a set of alpha parameters on the x-axis. The blue line represents the significance (-log10 p value; right y-axis) for each of the corresponding performance scores, derived from comparing to null models built from permuted samples (see Methods).

b, A grid showing the top cell populations from CITE-seq and flow cytometry (rows) whose baseline frequencies were selected by the models in (**a**) to predict the whole blood D1 – D0 Hallmark Interferon Gamma (IFNγ) Response module score at each of the alpha parameters (columns). The cell populations are ordered from top to bottom based on their significance at alpha = 0.7, which is the value that achieved the highest model significance in (**a**).

c, Similar to **(a)** but modeling the D1 – D0 serum IFNγ protein level as response.

d, Similar to **(b)** showing cell populations selected by the models in (**c**) to predict the D1 – D0 serum IFNγ protein level. Cell populations are ordered from top to bottom based on their significance at alpha = 0.4.

Supplementary Fig. 5

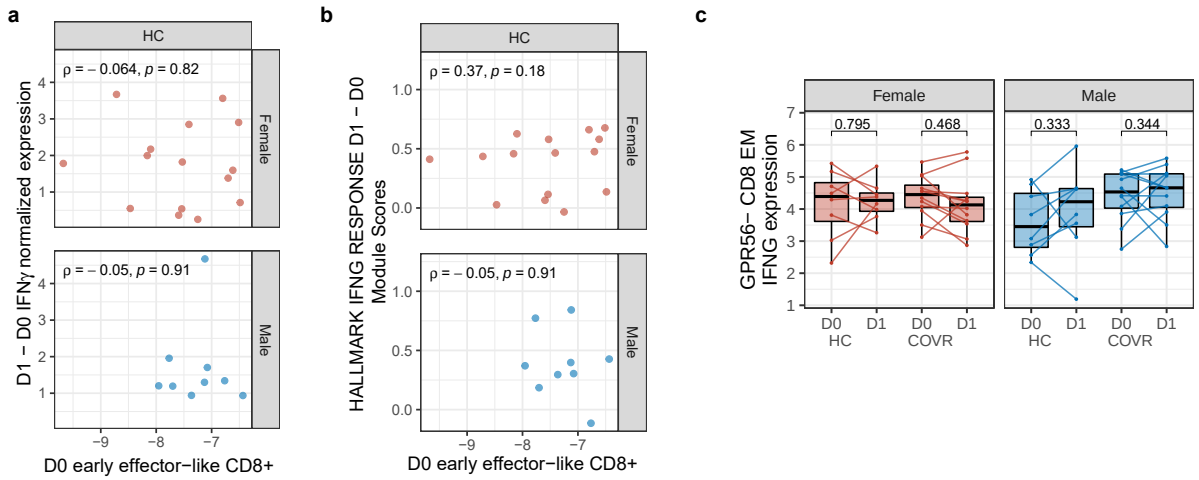

Supplementary Fig. 5. Additional supporting data for IFNγ responses by subsets of CD8+ EM T-cells.

a, Similar to Extended Data Fig. 4a, but for HC males and females.

b, Similar to Extended Data Fig. 4b, but for HC males and females.

c, Similar to Extended Data Fig. 4c, but for GPR56- (GPR56 negative) CD8 EM cells. All box plot elements are the same as indicated in Fig. 3. Unadjusted p values are shown.

Supplementary Fig. 6

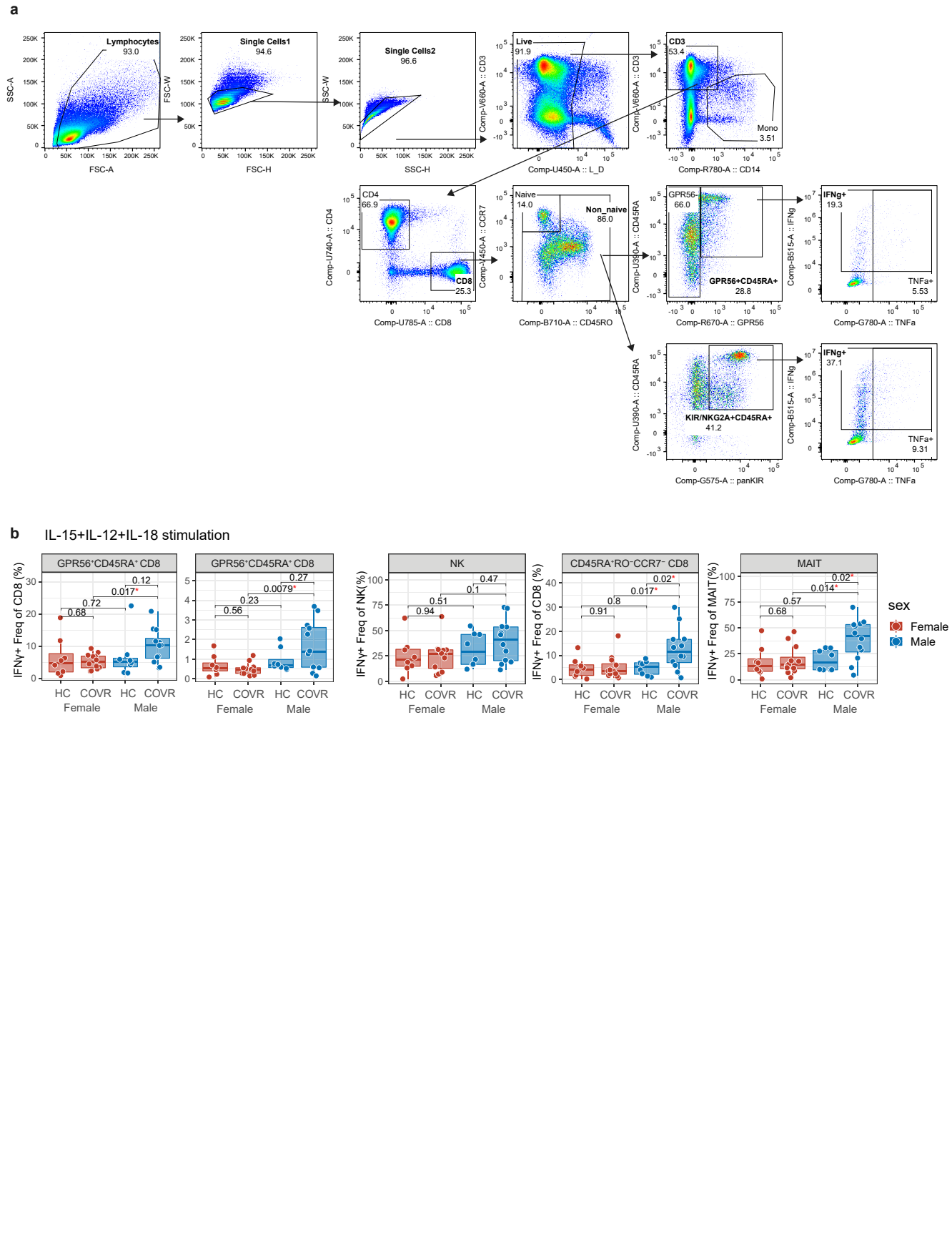

Supplementary Fig. 6. Flow cytometry analyses of *in vitro* cytokine stimulation of baseline PBMCs (D0 before influenza vaccination).

a, Gating strategies with IL-15 stimulation shown as an example.

b, Similar to Fig. 3i and Extended Data Fig. 4j, but showing the IFNγ^+ cells (as fraction of CD8+ T-cells) after stimulation by IL-15, IL-12, and IL-18 together (see Methods for details). All box plot elements are the same as indicated in Fig. 3. Unadjusted p values are shown.

Supplementary Fig. 7

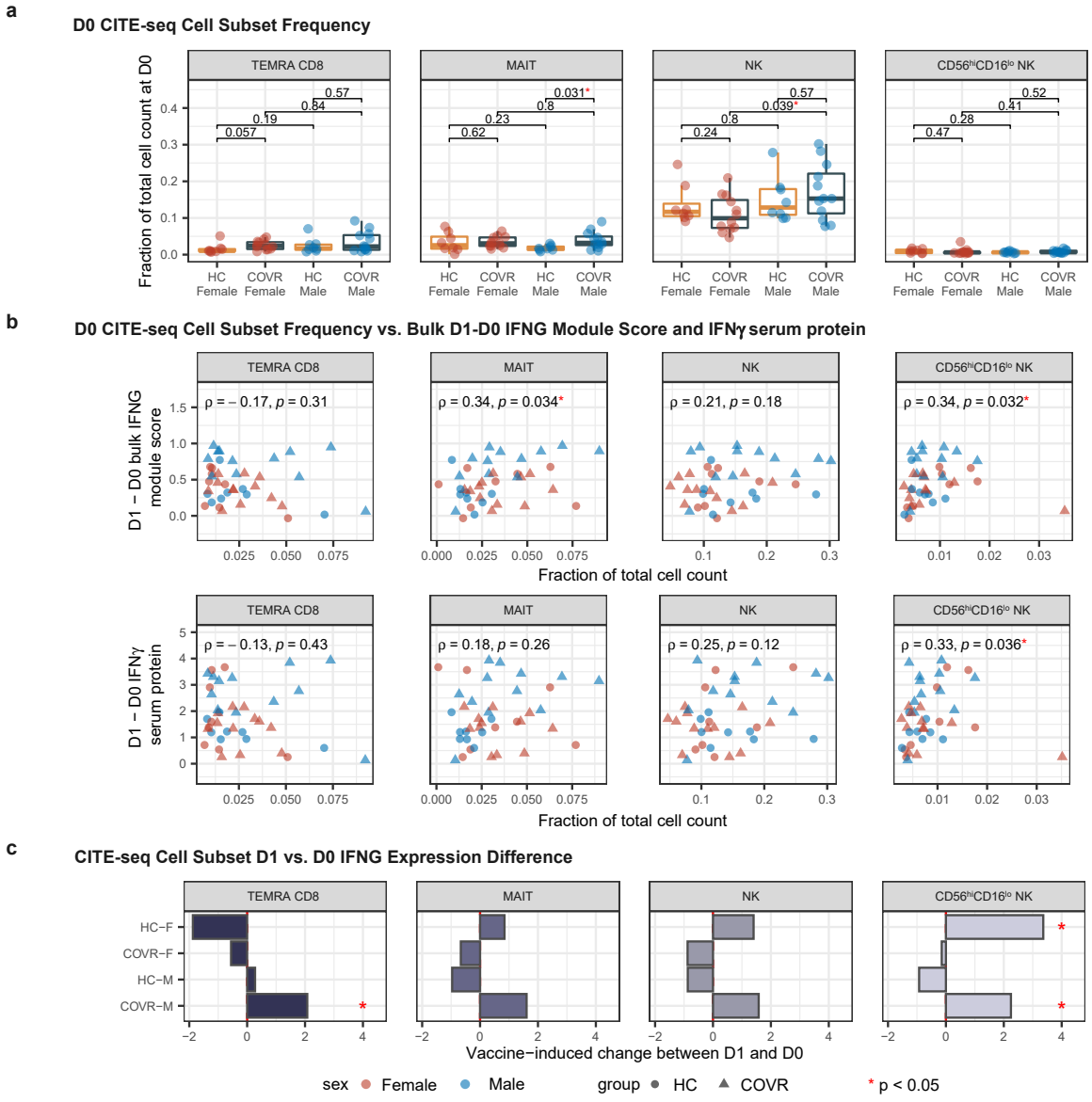

Supplementary Fig. 7. Additional cell subsets that potentially contribute to the increased day 1 IFNγ responses in COVID-19-recovered males.

a, Baseline frequencies (as fraction of total cells) of CD8 TEMRA, MAIT, NK, and $CD16^{lo}$ NK cells for HC-F (n=8), COVR-F (n=12), HC-M (n=8), and COVR-M (n=12). Significance of differences is determined by two-tailed Wilcoxon test.

b, Correlation between the baseline frequencies of the four populations in (**a**) and the D1 vs. D0 change of Hallmark IFNG response module scores and IFNγ serum protein levels for all subjects in the CITE-seq cohort – sample sizes indicated in (**a**). Spearman's rank correlation and unadjusted p values are shown.

c, Similar to Extended Data Fig. 4d but for each of the four cell populations listed in (**a**). All box plot elements are the same as indicated in Fig. 3.